

Control of entanglement and two-qubit quantum gates with atoms crossing a detuned optical cavity

D Gon \check{t} a¹ and S Fritzsche^{2,3}

¹ Max-Planck-Institut für Kernphysik,
P.O. Box 103980, D-69029 Heidelberg, Germany

² Gesellschaft für Schwerionenforschung (GSI),
D-64291 Darmstadt, Germany

³ Department of Physical Sciences,
P.O. Box 3000, Fin-90014 University of Oulu, Finland

E-mail: gonta@physi.uni-heidelberg.de

E-mail: s.fritzsche@gsi.de

Abstract. A scheme is proposed to generate an entangled state between two (Λ -type) four-level atoms that interact effectively by means of a detuned optical cavity and a laser beam that acts perpendicularly to the cavity axis. It is shown how the degree of entanglement for two atoms passing through the cavity can be controlled by manipulating their velocity and the (initial) distance between the atoms. In addition, three realistic schemes are suggested to implement the two-qubit gates within the framework of the suggested atom-cavity-laser setup, namely, the *i*-swap gate, controlled-Z gate, and the controlled- $\overline{\text{NOT}}$ gate. For all these schemes, we analyze and discuss the atomic velocities and inter-atomic distances for which these gates are realized most reliably.

PACS numbers: 42.50.Pq, 42.50.Dv, 03.67.Mn

1. Introduction

During recent years, quantum entanglement has been found important not only in studying the non-classical behavior of composite systems but also as one essential resource for the engineering and processing of quantum information. Nowadays, there are known various applications that (would) greatly benefit from having entangled quantum states available as, for instance, super-dense coding [1], quantum cryptography [2], or the use of Grover's quantum search algorithm [3], to name just a few of them. Despite of the recent progress in dealing with composite quantum systems, however, their manipulation and controlled interaction with the environment has remained a challenge for experiment until the present. Apart from various other implementations of composite systems, the proof for and an excellent control about the generation of entanglement has been achieved especially with neutral atoms that are coupled to high-finesse optical cavities [4, 5, 6].

From the experimental perspective, there are two basic types of (atomic) level configurations utilized to encode and store a single qubit: Apart from (i) the use of *optical* qubit, that simply refers to the two atomic levels separated by a optical transition frequency, one may (ii) utilize also the (so-called) *hyperfine* qubit that is associated with two hyperfine levels of—usually—the electronic ground state of the atom. In neutral atoms, these hyperfine levels are typically separated by a microwave frequency and are known to be robust with regard to decoherence effects and external stray fields in contrast to the optical qubits mentioned above. For the hyperfine qubits, therefore, rather long coherence times (~ 1 s) have been reported in the literature [7, 8, 9]. In addition, a number of microwave techniques have been developed during the last decades in order to initialize, manipulate and detect the state of such hyperfine qubits [7, 8, 9, 10, 11, 12].

Unfortunately, however, a hyperfine qubit cannot couple directly to a cavity with the resonant mode frequency in the optical domain. Therefore, in order to manipulate the information encoded by the atom, the superposition of the two hyperfine levels must first be transferred coherently to some other two (electronically) excited states before the atom enters the cavity, and this information must be brought back in a coherent fashion after the atom exits the cavity. Instead of an atomic two-level configuration, we then need to consider a four-level scheme, in which the two hyperfine levels for storing quantum information are associated with two (additional) optically excited levels. In order to realize an efficient atom-cavity coupling, moreover, the energy splitting of the two electronically excited levels should be compatible with the resonant frequency of the cavity. In this way, a coupling between the hyperfine qubit and the optical cavity can be achieved and might open a route towards the implementation of quantum gates via cavity-mediated atom-atom interactions.

The basic idea for the formation of entanglement between two four-level atoms that are coupled to a optical cavity and a external laser beam have been first suggested by You and co-authors [13], which follows the novel cavity-mediated atom-atom interaction regime from Ref. [14]. This interaction regime is based on the exchange of a photon between two bi-level atoms that is stimulated by a cavity which is detuned with regard to transition frequencies of the atoms. Later in Ref. [15], moreover, it was shown experimentally how this effective atom-atom interaction leads to the generation of entanglement between two atoms that cross a detuned microwave cavity. In the theoretical analysis of You *et al.*, however, it was assumed that both atoms couple to the same cavity mode via a constant coupling strength being independent

on the atomic position inside the cavity mode. In practice, the atoms cross the cavity one after another being separated by a macroscopic distance. This separation of the atoms implies that they have different atom-cavity couplings as given by the radiation pattern of the cavity mode standing-wave. Therefore, a more detailed description of the cavity-mediated entanglement formation has to be considered, in which the degree of entanglement between the atoms depends also on the atom-cavity coupling which depends, in turn, on the location of both atoms inside the cavity mode. Such a position-dependent coupling between the atoms and the cavity requires a revision of the previous theoretical analysis and suggests that the degree of entanglement, that is finally obtained, might depend substantially on the details of how the atoms cross the cavity in the course of interaction.

In the present work, we propose a scheme to generate an entangled state between the hyperfine qubits of two four-level atoms in a Λ -type level configuration. In this scheme, the interaction between the atoms is mediated by a optical cavity and a laser beam that acts perpendicularly to the cavity axis. In contrast to the analysis made by You *et al.*, moreover, we assume (i) the atoms to be separated from each other by a macroscopic distance such that *no direct* interaction between the atoms occurs and that (ii) both atoms interact simultaneously with the same cavity mode and laser field via a position-dependent couplings while passing through the cavity-laser setup. This scheme leads to an cavity-laser mediated *effective* atom-atom interaction, in which the two parameters to control this interaction are the velocity that encodes the atom-cavity interaction time, and the distance between the atoms that encodes the atom-cavity interaction strength. For two atoms being initially prepared in a product state (of their hyperfine qubits), we determine those velocities and distances for which the atoms become maximally entangled when passing through the proposed setup. Apart from generating entanglement between the atoms, we also suggest schemes to implement various two-qubit quantum logical gates, such as the i-swap gate, controlled-Z gate, and controlled- $\overline{\text{NOT}}$ gate. All these gates can be implemented within the given framework, and the respective velocity and inter-atomic distance of the atoms are discussed, for which the gate fidelities become maximal.

The paper is organized as follows. In the next section, we introduce the scheme to entangle the hyperfine qubits of two four-level atoms. This includes the theoretical description of the effective atom-atom interaction evolution that allows to control this interaction in practice. In Sec. 2.1, in particular, we present and explain all the steps necessary within the proposed (experimental) set-up, while a more detailed view on this effective interaction is given in Sec. 2.2 by using the adiabatic elimination procedure. In Sec. 3, then, the schemes for the implementation of the i-swap, controlled-Z, and controlled- $\overline{\text{NOT}}$ gates are presented and discussed. A few conclusions are finally given in Sec. 4.

2. Generation of the Two-Atom Entanglement via Optical Cavity

In this section, we propose and explain our scheme to entangle the hyperfine qubits of two four-level atoms if they were initially prepared in a product state. We hereby assume that the atoms can be controlled with regard to their separation and velocity when they enter the experimental setup that is displayed in Fig. 1(c).

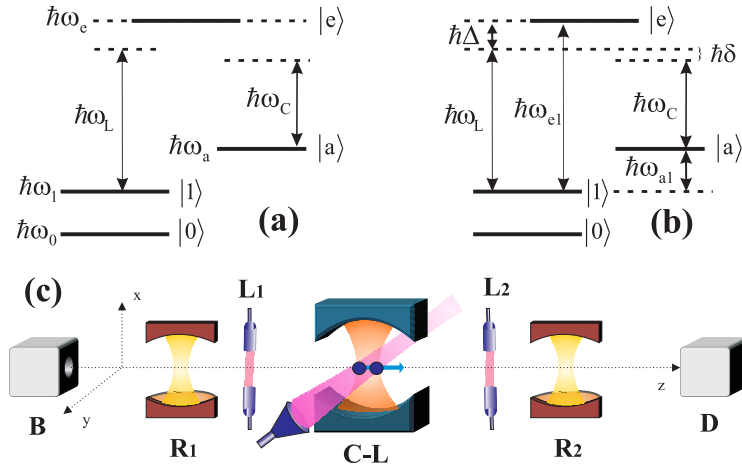


Figure 1. (Color online) The atomic four-level Λ -type configuration in (a) the Schrödinger picture and (b) the interaction picture. (c) Schematic setup of the experiment. Two neutral atoms from a source B are supposed to pass through a Ramsey zone R_1 , a pair of Raman laser beams L_1 , an optical cavity C with a perpendicularly acting laser beam L as well as through a second pair of Raman lasers L_2 and Ramsey zone R_2 , before the hyperfine states of the atoms is detected at the detector D .

2.1. Off-Resonant Atom-Cavity interaction

Let us start by considering an atom in the Λ -type four-level configuration as displayed in Fig. 1(a). In this level configuration, the two (hyperfine) states $|0\rangle$ and $|1\rangle$ of the atomic ground levels carry the qubit information and are supplemented by the two electronically excited states $|a\rangle$ and $|e\rangle$ that are separated from each other by an optical transition frequency. Below, we assume to have two identical atoms A_1 and A_2 in such a Λ -type configuration that are initially prepared in the composite state $|0, \bar{1}\rangle \equiv |0\rangle \times |\bar{1}\rangle$, where the bar in $|\bar{a}\rangle$ refers to the state of atom A_2 . In addition, the atoms are separated by a macroscopic distance ℓ being large enough such that they do not interact directly with each other and both atoms move with the same (constant) velocity \vec{v} along the z axis [see Fig. 1(c)]. Before atom A_1 enters the cavity, its electronic population is transferred from state $|0\rangle$ to the state $|a\rangle$ by using a pair of slightly off-resonant laser beams which are coupled to the atomic transitions $|0\rangle \leftrightarrow |e\rangle$ and $|e\rangle \leftrightarrow |a\rangle$, respectively. Such a population transfer is known as the two-photon Raman process [16] that enables one to perform a second-order transition between the states $|0\rangle$ and $|a\rangle$. For instance, this could be done by utilizing a two phase-locked laser diode [11]. Below, we shall refer to this population transfer briefly as a Raman pulse and will distinguish between the Raman pulses (laser beams) L_1 and L_2 in front and behind the cavity [see Fig. 1(c)]; also in the temporal diagram from Fig. 2, these Raman pulses are displayed as boxed pink circles. We assume, therefore, that the purpose of these Raman pulses is just to transfer the electronic population from hyperfine state $|0\rangle$ to the optical level $|a\rangle$ in the zone L_1 , and back from $|a\rangle$ to $|0\rangle$ in zone L_2 . The same Raman pulses are applied also to the atom A_2 which follows A_1 subsequently with distance ℓ . However, since the second atom enters the set-up in the state $|\bar{1}\rangle$, it remains unaffected by the Raman pulse L_1 and, thus, the two atoms

enter the cavity in the product state $|a, \bar{1}\rangle$.

Inside the cavity, both atoms A_1 and A_2 couple via the optical transition $|a\rangle \leftrightarrow |e\rangle$ (and $|\bar{a}\rangle \leftrightarrow |\bar{e}\rangle$, respectively) to the same cavity mode with the resonant frequency ω_C [see Fig. 1(a)]. As we discussed above, a revised description of the atom-cavity interaction evolution is based on the position-dependent atom-cavity coupling

$$g(\vec{r}) = g_o \exp(-|\vec{r}|^2/w^2), \quad (1)$$

where g_o denotes the vacuum Rabi frequency and w the (so-called) cavity mode waist that is the minimum width of the radiation pattern given by the cavity mode standing-wave. For the two atoms which move through the cavity with the velocity \vec{v} along the z axis, the Gaussian profile (1) gives rise to the time-dependent atom-cavity couplings $g_1(t) \equiv g(z_1^o + vt)$ and $g_2(t) \equiv g(z_2^o + vt)$, and where $z_1^o - z_2^o = \ell > 0$ denotes the initial distance between the atoms.

The cavity-mediated atom-atom interaction (i.e., without the laser beam L) is based on the stimulated exchange of a *single* photon between two atoms prepared in the product state $|a, \bar{e}\rangle$. This photon exchange can be understood as the emission of a virtual photon into the cavity mode by the atom A_2 and the re-absorption of the photon by the atom A_1 , while both atoms are coupled off-resonantly to the same cavity mode. An off-resonant atom-cavity interaction hereby refers to the case when the difference (or detuning) between the atomic $|a\rangle \leftrightarrow |e\rangle$ transition frequency and the frequency of the cavity mode ω_L is large enough: $|\omega_C - (\omega_e - \omega_a)| \gg |g_\mu(t)|$, so that only a virtual atom-cavity energy exchange can occur [14].

In our present scheme, in contrast, the atoms enter the cavity in the composite state $|a, \bar{1}\rangle$, and hence a further intermediate process $|a, \bar{1}\rangle \rightarrow |a, \bar{e}\rangle$ is first necessary to obtain the state $|a, \bar{e}\rangle$ that could evolve into $|e, \bar{a}\rangle$ by means of the detuned cavity. For this reason, the atoms are exposed to a laser beam that acts transversally to the cavity axis and *in addition* to their interaction with the cavity mode [see Fig. 1(c)]. The laser given by the frequency ω_L couples the atomic transitions $|1\rangle \leftrightarrow |e\rangle$ and $|\bar{1}\rangle \leftrightarrow |\bar{e}\rangle$, respectively, as shown in Fig. 1(a). The position-dependent atom-laser coupling $\Omega(\vec{r}) = \Omega_o \exp(-|\vec{r}|^2/\tilde{w}^2)$ hereby implies the time-dependent couplings for each atom, namely $\Omega_1(t) \equiv \Omega(z_1^o + vt)$ and $\Omega_2(t) \equiv \Omega(z_2^o + vt)$, and where the waist of the atom-laser coupling \tilde{w} is assumed to be much larger than for the cavity mode. With the above couplings of the atoms to both, the laser and the cavity mode, the atomic composite state can be manipulated in order to create an energy exchange between $|a, \bar{1}\rangle$ and $|1, \bar{a}\rangle$ in a similar way as have been suggested by You and coworkers. This exchange is based on the sequence of four steps

$$|a, \bar{1}; n\rangle \rightarrow |a, \bar{e}; n\rangle \begin{array}{l} \nearrow |a, \bar{a}; n+1\rangle \\ \searrow |e, \bar{e}; n-1\rangle \end{array} \begin{array}{l} \searrow |e, \bar{a}; n\rangle \\ \nearrow |1, \bar{a}; n\rangle \end{array}, \quad (2)$$

if there were n photons initially in the cavity mode. As seen above, this sequence contains in its middle part a virtual process in which a photon is emitted by the first and absorbed by the second atom, so that the final state of the atoms is independent of the number of cavity photons. For an initially empty cavity, we can therefore simplify the above sequence to

$$|a, \bar{1}; 0\rangle \rightarrow |a, \bar{e}; 0\rangle \rightarrow |a, \bar{a}; 1\rangle \rightarrow |e, \bar{a}; 0\rangle \rightarrow |1, \bar{a}; 0\rangle. \quad (3)$$

Therefore, if we omit to display the intermediate states in the sequence (3), the laser and cavity field together produce an *effective* atom-atom interaction evolution

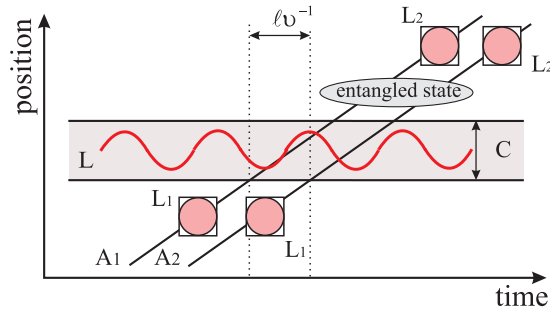


Figure 2. (Color online) Temporal sequence of steps that need to be carried out in order to generate an entangled state for the two hyperfine qubits of atoms A_1 and A_2 . The grey rectangular area C denotes the spatial extent of the cavity. The (pink) boxed circles, denoted as L_1 and L_2 , refer to the two (pairs of) Raman laser beams in front and behind the cavity. The two atomic qubits are entangled with each other when both atoms have left the cavity.

$|a, \bar{1}\rangle \xrightarrow{L, C} |1, \bar{a}\rangle$ in which the state of the cavity field is factorized out in the vacuum state. By exploiting this effective evolution, the maximally entangled state

$$|\Phi\rangle = \frac{1}{\sqrt{2}} (|a, \bar{1}\rangle + e^{i\varphi}|1, \bar{a}\rangle), \quad (4)$$

where $e^{i\varphi}$ is a constant phase factor, can be generated by tuning the atomic velocity v and the inter-atomic distance ℓ for a given set of cavity-laser parameters: ω_C , ω_L , w , g_o , and Ω_o . In the next subsection, we shall analyze in more details how this effective atom-atom interaction depends on the velocity and distance of the atoms, while both atoms are passing through the setup.

After both the atoms A_1 and A_2 have left the cavity, the electronic population of the excited states $|a\rangle$ and $|\bar{a}\rangle$ is coherently transferred back to the (ground) hyperfine levels $|0\rangle$ and $|\bar{0}\rangle$ in order to protect them from the spontaneous decay of these levels. As before, this is achieved by applying a Raman pulse L_2 behind the cavity [see Fig. 1(c)]. The entangled state (4) is then mapped onto the state

$$|\Phi'\rangle = \frac{1}{\sqrt{2}} (|0, \bar{1}\rangle + e^{i\varphi}|1, \bar{0}\rangle). \quad (5)$$

All the manipulations with the atoms which we have just described are summarized graphically in Fig. 2, in which the spatio-temporal evolution of the atoms and the cavity is displayed.

2.2. Time-Evolution of the Effective Atom-Atom Interaction

While the sequence (3) provides the basic idea of how an effective coupling can be achieved between the atoms, we need to analyze this sequence in more details as to understand how to control this coupling in practice. For this purpose, we shall use the *adiabatic elimination* procedure (see Refs. [17, 14] and Ref. [18] for another derivation) which enables one to exclude all the intermediate degrees of freedom due to the action of the cavity mode and the laser field.

Formally, the time evolution of the coupled atom-cavity-laser system is driven by the Hamiltonian

$$H = H_1 + H_2 + H_C, \quad (6)$$

where ($\hbar = 1$, $\mu = 1, 2$)

$$H_\mu = \omega_1 |1\rangle_\mu \langle 1| + \omega_e |e\rangle_\mu \langle e| + \omega_a |a\rangle_\mu \langle a| \\ + \frac{1}{2} [\Omega_\mu(t) e^{-i\omega_L t} |e\rangle_\mu \langle 1| + g_\mu(t) c |e\rangle_\mu \langle a| + h.c.];$$

describes the atom A_μ and its interaction with the cavity and laser field, and where

$$H_C = \omega_C c^\dagger c, \quad (7)$$

refers to the cavity mode energy. In the atomic Hamiltonian (6), hereby $\hbar\omega_1$, $\hbar\omega_e$, and $\hbar\omega_a$ are the (excitation) energies of atomic states $|1\rangle$, $|e\rangle$ and $|a\rangle$ [see Fig. 1(a)], while c and c^\dagger denote the annihilation and creation operators for a photon in the cavity mode which act upon the Fock states $|n\rangle$.

In order to simplify the evaluation of the Schrödinger equation that is associated with the Hamiltonian (6), let us switch here to the interaction picture given by [13]

$$U_{int}^0 = e^{-i(\omega_1 + \omega_L)t} \sum_\mu |e\rangle_\mu \langle e| e^{-i\omega_1 t} \sum_\mu |1\rangle_\mu \langle 1| \times \\ e^{-i\omega_a t} \sum_\mu |a\rangle_\mu \langle a| e^{-i[\omega_L - (\omega_a - \omega_1)]t} c^\dagger c. \quad (8)$$

In this picture, the atom-cavity-laser interaction Hamiltonian becomes

$$H_{int} = -\delta c^\dagger c + \Delta \sum_\mu |e\rangle_\mu \langle e| \\ + \frac{1}{2} \sum_\mu [\Omega_\mu(t) |e\rangle_\mu \langle 1| + g_\mu(t) c |e\rangle_\mu \langle a| + h.c.], \quad (9)$$

where $\Delta = \omega_{e1} - \omega_L$ and $\delta = \omega_L - \omega_C - \omega_{a1} = (\omega_{ea} - \omega_C) - (\omega_{e1} - \omega_L)$ refer to the off-resonance shifts (detuning) of the laser and cavity frequencies as depicted in Fig. 1(b).

The Hamiltonian (9) drives the state of the composite atom-cavity-laser system due to the Schrödinger equation

$$i \frac{d|\Psi(t)\rangle}{dt} = H_{int} |\Psi(t)\rangle, \quad (10)$$

where the (composite) wave function $|\Psi(t)\rangle$ is defined in the product space of three (sub)systems: $A_1(|1\rangle, |e\rangle, |a\rangle)$, $A_2(|\bar{1}\rangle, |\bar{e}\rangle, |\bar{a}\rangle)$, and the cavity Fock states $C(|0\rangle, |1\rangle)$. Moreover, by taking into account the composite states that occur in sequence (3), we may restrict this wave function to the subspace

$$|\Psi(t)\rangle = C_1(t) |a, \bar{1}; 0\rangle + C_2(t) |a, \bar{e}; 0\rangle + C_3(t) |a, \bar{a}; 1\rangle \\ + C_4(t) |e, \bar{a}; 0\rangle + C_5(t) |1, \bar{a}; 0\rangle, \quad (11)$$

for which the Schrödinger equation (10) gives rise to the set of closed equations

$$i \dot{C}_1(t) = \frac{1}{2} \Omega_2(t) C_2(t), \quad (12a)$$

$$i \dot{C}_2(t) = \Delta C_2(t) + g_2(t) C_3(t) + \frac{1}{2} \Omega_2(t) C_1(t), \quad (12b)$$

$$i \dot{C}_3(t) = -\delta C_3(t) + g_1(t) C_4(t) + g_2(t) C_2(t), \quad (12c)$$

$$i\dot{C}_4(t) = \Delta C_4(t) + g_1(t)C_3(t) + \frac{1}{2}\Omega_1(t)C_5(t), \quad (12d)$$

$$i\dot{C}_5(t) = \frac{1}{2}\Omega_1(t)C_4(t), \quad (12e)$$

and where the dot denotes the time derivative.

The off-resonant regime of the atom-cavity and atom-laser interactions, we assumed, implies

$$|\delta| \gg |g_\mu(t)|, \quad |\Delta| \gg |\Omega_\mu(t)|, \quad |\delta\Delta| \gg |g_\mu^2(t)|. \quad (13)$$

These conditions, therefore, justify the adiabatic elimination procedure for a sufficiently slow-varying time-dependent atom-cavity $g_\mu(t)$ and atom-laser coupling $\Omega_\mu(t)$. The adiabatic elimination procedure implies the vanishing of the time derivatives $\dot{C}_2(t)$, $\dot{C}_3(t)$, and $\dot{C}_4(t)$, which together with the conditions (13) lead to the exclusion of the Eqs. (12b)-(12d) that account for the evolution of the state vectors $|a, \bar{e}; 0\rangle$, $|a, \bar{a}; 1\rangle$, and $|e, \bar{a}; 0\rangle$, respectively. Here, we shall omit the details of the derivation for which the reader is referred to the literature [13, 17, 14, 18]. The remaining Eq. (12a) and Eq. (12e) for the functions $C_1(t)$ and $C_2(t)$ take the closed form

$$i\dot{C}_1(t) = -\frac{\Omega_2^2(t)}{4\Delta}C_1(t) + \lambda(t)C_5(t), \quad (14a)$$

$$i\dot{C}_5(t) = \lambda(t)C_1(t) - \frac{\Omega_1^2(t)}{4\Delta}C_5(t), \quad (14b)$$

where

$$\lambda(t) = \frac{\Omega_1(t)\Omega_2(t)g_1(t)g_2(t)}{4\delta\Delta^2} \quad (15)$$

is the effective coupling between the initial and final composite states $|a, \bar{1}; 0\rangle$ and $|1, \bar{a}; 0\rangle$, respectively.

The atom-laser coupling $\Omega_\mu(t)$ is determined by the interaction of the electric-dipole of the atom with the electric field of the laser. However, since the waist of the laser beam is assumed to be much larger than those of the cavity mode, we may take $\Omega_\mu(t) = \Omega = \text{const.}$ and include the time-variation only due to the atom-cavity coupling $g_\mu(t)$. With this simplification in mind, an analytical solution of Eqs. (14a)-(14b) can be obtained in the form

$$|\Psi(t)\rangle = e^{i\frac{\Omega^2}{4\Delta}t}|\Phi(t)\rangle \quad (16)$$

with

$$|\Phi(t)\rangle = \cos\xi(t)|a, \bar{1}\rangle - i\sin\xi(t)|1, \bar{a}\rangle, \quad (17)$$

if the wave-function $|\Psi(t)\rangle$ was prepared initially in the product state $|a, \bar{1}; 0\rangle$. In the expression (17), moreover, the cavity field state is not shown as being factorized out in the vacuum state and the effective atom-atom *coupling angle* is given by

$$\xi(t) = \int_{-\infty}^t \lambda(s) ds. \quad (18)$$

The wave function (17) describes an entangled state for the atoms A_1 and A_2 , whose time evolution can be obtained also from the effective Hamiltonian

$$H_{eff} = \lambda(t) (\sigma_1^- \sigma_2^+ + \sigma_1^+ \sigma_2^-), \quad (19)$$

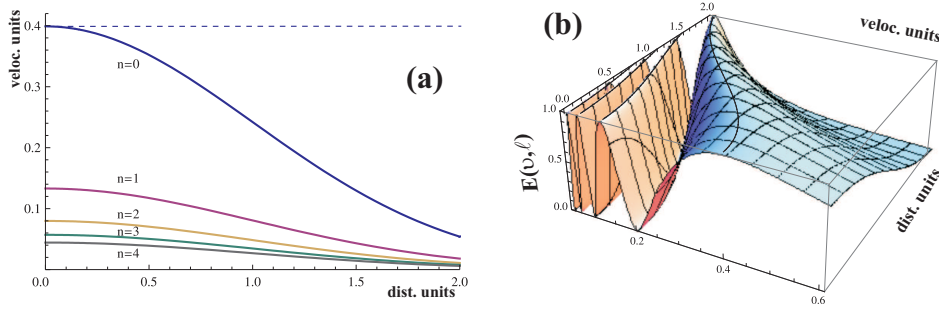


Figure 3. (Color online) (a) Atomic velocities v and inter-atomic distances ℓ for which the initial product state $|a, \bar{1}\rangle$ becomes maximally entangled due to the cavity-laser mediated atom-atom interaction. The velocity v is displayed in units of $\Omega^2 g_o^2 w / \delta \Delta^2$ and the inter-atomic distance in units of w . Along the lines, the condition $\theta(v, \ell) = (2n+1)\pi/4$ is satisfied for the asymptotic couplings angle with $n = 0, 1, 2, 3, 4$. The straight dashed line corresponds to a vanishing inter-atomic distance, which is obtained in the formal limit $\ell \rightarrow 0$ for $n = 0$. (b) Von Neumann entropy $E(v, \ell)$ as function of the atomic velocity v and inter-atomic distance ℓ (using the same units).

where $\sigma_\mu^+ = |1\rangle_\mu \langle a|$ and $\sigma_\mu^- = |a\rangle_\mu \langle 1|$ denote the two-photon atomic excitation and de-excitation operators. Owing to its obvious simplicity, this Hamiltonian provides a much better understanding of the effective two-atom evolution (17) that is mediated by the cavity-laser fields and by using the ansatz (11) within the adiabatic regime. Below, we shall restrict ourselves to the evolution of the function $|\Phi(t)\rangle$ since the Hamiltonian that drives the wave function $|\Psi(t)\rangle$ differs from (19) by just the constant term $H_0 = \frac{\Omega^2}{4\Delta} (|1\rangle\langle 1| + |\bar{1}\rangle\langle \bar{1}|)$. This factor need not to be considered since we could utilize a modified interaction picture given by the unitary transformation $U_{int}^1 = \exp(i H_0 t)$, for which the (original) wave function (16) would coincide with (17).

When both atoms have left the cavity (which is formally obtained in the limit $t \rightarrow +\infty$), the state (17) becomes

$$|\Phi_{+\infty}\rangle = \cos \theta(v, \ell) |a, \bar{1}\rangle - i \sin \theta(v, \ell) |1, \bar{a}\rangle, \quad (20)$$

and where the asymptotic coupling angle is given by

$$\theta(v, \ell) \equiv \xi(+\infty) = \sqrt{\frac{\pi}{32}} \frac{\Omega^2 g_o^2 w}{\delta \Delta^2 v} \exp\left(-\frac{\ell^2}{2w^2}\right). \quad (21)$$

Note that according to our scheme in Fig. 2, the atomic states $|a\rangle$ and $|\bar{a}\rangle$ are mapped onto the hyperfine states $|0\rangle$ and $|\bar{0}\rangle$ by applying a Raman pulse L_2 shortly after the atoms have crossed the cavity. Therefore, the wave-function (20) becomes

$$|\Phi'_{+\infty}\rangle = \cos \theta(v, \ell) |0, \bar{1}\rangle - i \sin \theta(v, \ell) |1, \bar{0}\rangle. \quad (22)$$

From Eq. (22), we can easily read off the condition: $\theta(v, \ell) = (2n+1)\pi/4$, with n being an integer, for which the two atoms become maximally entangled with each other initially being prepared in the product state $|a, \bar{1}\rangle$. For fixed cavity-laser parameters (δ , Δ , w , g_o and Ω), this condition implies that the values of atomic velocity v and inter-atomic distances ℓ cannot be chosen arbitrarily but must follow the (so-called) *lines of maximal entanglement* displayed in Fig. 3(a) for $n = 0, 1, 2, 3, 4$. According

to this figure, the change between the (maximally) entangled and disentangled state occurs more and more rapidly as the velocity is decreased (or n increases). In Fig. 3(a), all velocities are given in units of $\Omega^2 g_o^2 w / \delta \Delta^2$ and all distances in units of the cavity waist w . For typical atom-cavity-laser parameters: $\delta = 360$ MHz, $\Delta = 380$ MHz, $g_o = 27$ MHz, $\Omega = 50$ MHz, and $w = 13 \mu\text{m}$, these velocity and distance units take the values of 0.46 m/s and $13 \mu\text{m}$, respectively. These values are compatible with the velocities in the range $0.01, \dots, 1$ m/s which were utilized in the recent cavity QED experiments [19, 20, 21], in which atoms are coherently transported inside the cavity by means of a optical lattice trap (see below).

Next, let us analyze how the degree of entanglement depends on the velocity v and distance ℓ of the atoms. For this reason we display in Fig. 3(b) the *von Neumann entropy* [22]

$$\begin{aligned} E(v, \ell) &\equiv -\text{Tr}[\rho(v, \ell) \log_2 \rho(v, \ell)] \\ &= -\cos^2 \theta(v, \ell) \log_2 [\cos^2 \theta(v, \ell)] \\ &\quad - \sin^2 \theta(v, \ell) \log_2 [\sin^2 \theta(v, \ell)], \end{aligned} \quad (23)$$

where $\rho(v, \ell) = \text{Tr}_2(|\Phi'_{+\infty}\rangle\langle\Phi'_{+\infty}|)$ denotes the reduced density operator of the first hyperfine qubit [see Eq. (22)]. The maximal values of the von Neumann entropy, i.e., $E(v, \ell) = 1$, are obtained for the velocities and distances as displayed in Fig. 3(a). Moreover, as seen from Fig. 3(b), the velocities and distances along the (blue) $n = 0$ line from Fig. 3(a) appear to be the most appropriate for any practical implementation of this scheme, since for these values of v and ℓ , the obtained entanglement is less sensitive with regard to small uncertainties. This leads us to the conclusion that the v and ℓ combinations along this line ($n = 0$) might be relevant for experimental attempts to generate the atom-atom entanglement by means of the suggested setup.

Since the atom-atom interaction sequence (3) can be easily time reversed to

$$|1, \bar{a}; 0\rangle \rightarrow |e, \bar{a}; 0\rangle \rightarrow |a, \bar{a}; 1\rangle \rightarrow |a, \bar{e}; 0\rangle \rightarrow |a, \bar{1}; 0\rangle \quad (24)$$

we can generate also the state ($t \rightarrow +\infty$)

$$|\tilde{\Phi}_{+\infty}\rangle = \cos \theta(v, \ell) |1, \bar{a}\rangle - i \sin \theta(v, \ell) |a, \bar{1}\rangle, \quad (25)$$

from the atoms initially being prepared in the product state $|1, \bar{a}\rangle$. Together with the Raman pulse L_2 that maps back the atomic states $|a\rangle \rightarrow |0\rangle$ and $|\bar{a}\rangle \rightarrow |\bar{0}\rangle$, we then obtain the state

$$|\tilde{\Phi}'_{+\infty}\rangle = \cos \theta(v, \ell) |1, \bar{0}\rangle - i \sin \theta(v, \ell) |0, \bar{1}\rangle. \quad (26)$$

For the other two initial (product) states $|a, \bar{a}\rangle$ and $|1, \bar{1}\rangle$, in contrast, no effective interaction occurs on the atoms when they pass through the cavity-laser system. From this fact and Eqs. (20), (25), we conclude that the effective Hamiltonian (19) gives a complete description of the (effective) atom-atom interaction for all four possible initial product states of the two atoms being mediated by the cavity-laser fields in the adiabatic regime.

3. Two-Qubit Quantum Logic Gates

In the previous section, we have shown how the atomic hyperfine qubits of the two atoms A_1 and A_2 can be manipulated adiabatically by means of the cavity-laser setup from Fig. 1(c) and the sequence of steps from Fig. 2. Independent of the initial state of the qubits, the evolution of the two-qubit hyperfine input state $|\psi_{in}\rangle = \sum_i c_i^o |\mathbf{v}_i\rangle$

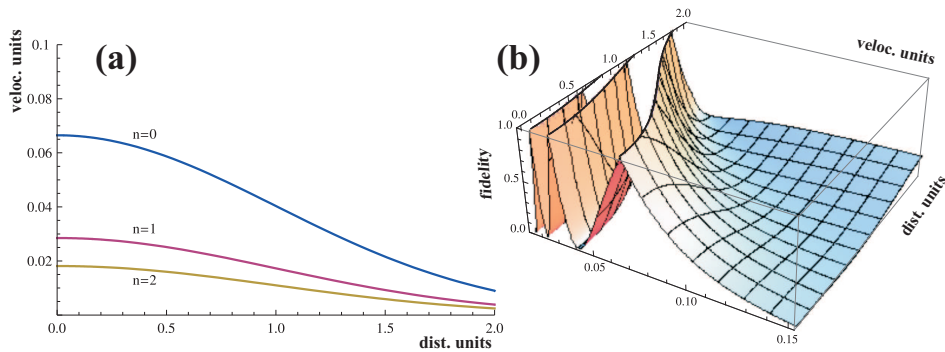


Figure 4. (Color online) (a) Combinations of the atomic velocity v and inter-atomic distance ℓ that realizes the i-swap gate (29), i.e., for which the condition (30) is fulfilled for $n = 0, 1, 2$. (b) Fidelity $F_{i\text{-swap}}(v, \ell)$ as function of the atomic velocity v and inter-atomic distance ℓ . The same units of v and ℓ are used as in Fig. 3.

into the output state $|\psi_{out}\rangle = \sum_i c_i(v, \ell) |\mathbf{v}_i\rangle$ ($i, j = 1, \dots, 4$) is given by the unitary matrix

$$U_{ij}(v, \ell) = \begin{pmatrix} 1 & 0 & 0 & 0 \\ 0 & \cos \theta(v, \ell) & -i \sin \theta(v, \ell) & 0 \\ 0 & -i \sin \theta(v, \ell) & \cos \theta(v, \ell) & 0 \\ 0 & 0 & 0 & 1 \end{pmatrix} \quad (27)$$

expressed in the two-qubit hyperfine basis

$$|\mathbf{v}_1\rangle = |0, \bar{0}\rangle, |\mathbf{v}_2\rangle = |0, \bar{1}\rangle, |\mathbf{v}_3\rangle = |1, \bar{0}\rangle, |\mathbf{v}_4\rangle = |1, \bar{1}\rangle, \quad (28)$$

and where $c_i(v, \ell) = \sum_j U_{ij}(v, \ell) c_j^o$. For different values of the atomic velocity v and inter-atomic distance ℓ , different transformations are therefore realized including, for instance, the generation of maximally entangled state (5) if one starts from the initial product state $|0, \bar{1}\rangle$. Moreover, we can analyze the atom-atom coupling angle $\theta(v, \ell)$ for different combinations of v and ℓ and for its capability to realize non-trivial two-qubit quantum gates. In fact, the suggested set-up is suitable for realizing the i-swap, controlled-Z, and the controlled- $\overline{\text{NOT}}$ quantum gates for different choices of the velocity and distance, together with some minor modifications in the steps that are necessary to prepare the atoms before (afterwards) they enter (leave) the cavity-laser system (see below). In the following, we consider these gates in more details and display their temporal diagrams and possible values (v, ℓ) for which these gates are realized.

3.1. i-Swap Gate

Perhaps the simplest quantum gate is the i-swap gate [23] which is expressed in the atomic basis (28) as

$$U_{ij}^{i\text{-swap}} = \begin{pmatrix} 1 & 0 & 0 & 0 \\ 0 & 0 & i & 0 \\ 0 & i & 0 & 0 \\ 0 & 0 & 0 & 1 \end{pmatrix}. \quad (29)$$

By comparing the Eqs. (27) and (29), we see that this gate can be generated whenever the effective coupling angle fulfills the condition

$$\theta(v, \ell) = 3\pi/2 + 2\pi n. \quad (30)$$

The Fig. 4(a) displays combinations of the atomic velocity v and the inter-atomic distance ℓ which satisfy this condition for $n = 0, 1, 2$. For the i-swap gate, moreover, the sequence of steps that needs to be carried out before and after the atoms have crossed the cavity is the same as shown in Figure 2 and no additional manipulations are required in order to implement this gate.

From the viewpoint of an experiment, as we have discussed, it is important to know how stable a gate operation can be performed for small deviations in the (v, ℓ) parameters. This stability can be seen from the fidelity (distance) between the i-swap gate (29) and the unitary matrix (27) obtained for different values of (v, ℓ) . The Fig. 4(b) displays such a fidelity that we have defined as

$$\begin{aligned} F_{i\text{-swap}}(v, \ell) &\equiv 1 - \mathcal{N}(\|U(v, \ell) - U^{i\text{-swap}}\|) \\ &= 1 - \sqrt{\frac{1 + \sin \theta(v, \ell)}{2}}, \end{aligned} \quad (31)$$

where $\|M\| \equiv \sqrt{\text{Tr}(MM^+)}$ is the *Frobenius* norm [24] and $\mathcal{N}(f_{v,\ell}) \equiv f_{v,\ell} \cdot (\text{Max}(f_{v,\ell}))^{-1}$ is used for its normalization upon the interval $0 \leq F_{i\text{-swap}} \leq 1$.

By construction, this fidelity is a continuous function for which the realization of the i-swap gate occurs when $F_{i\text{-swap}}(v, \ell) = 1$, which corresponds to the values (v, ℓ) displayed in Fig. 4(a).

3.2. Controlled-Z Gate

For two interacting qubits A and B , the controlled-Z gate is defined by the transformation [22]

$$U_{CZ}|\alpha_A, \beta_B\rangle = (-1)^{\alpha\beta}|\alpha_A, \beta_B\rangle, \quad (32)$$

where $\alpha, \beta = 0, 1$ are the basis states. This gate is a simple example of the conditional quantum dynamics which introduces an additional phase $e^{i\pi} = -1$ whenever both qubits are in the state $|1_A, 1_B\rangle$.

In Sec. 2, we concluded that the initial product state $|1, \bar{1}\rangle$ of the two atoms does not undergo any evolution mediated by the cavity-laser fields. Therefore, the direct identification of the atomic hyperfine states $|0\rangle, |1\rangle$ and $|\bar{0}\rangle, |\bar{1}\rangle$ with the (logical) qubit states $|0_A\rangle, |1_A\rangle$ and $|\bar{0}_B\rangle, |\bar{1}_B\rangle$ in (32) will not allow us to realize the control-Z gate, while the reversed assignment for the qubit A

$$|0\rangle = |1_A\rangle, \quad |1\rangle = |0_A\rangle, \quad |\bar{0}\rangle = |0_B\rangle, \quad |\bar{1}\rangle = |1_B\rangle. \quad (33)$$

would do so. With this assignment of the basis (28), the transformation matrix for the requested controlled-Z gate becomes

$$U_{ij}^{CZ} = \begin{pmatrix} 1 & 0 & 0 & 0 \\ 0 & -1 & 0 & 0 \\ 0 & 0 & 1 & 0 \\ 0 & 0 & 0 & 1 \end{pmatrix}. \quad (34)$$

In contrast to the i-swap gate (29), however, the matrix (34) cannot be obtained from the evolutionary matrix (27) by just imposing a condition of the type (30) on the coupling angle $\theta(v, \ell)$. Instead we must consider here the new temporal diagram

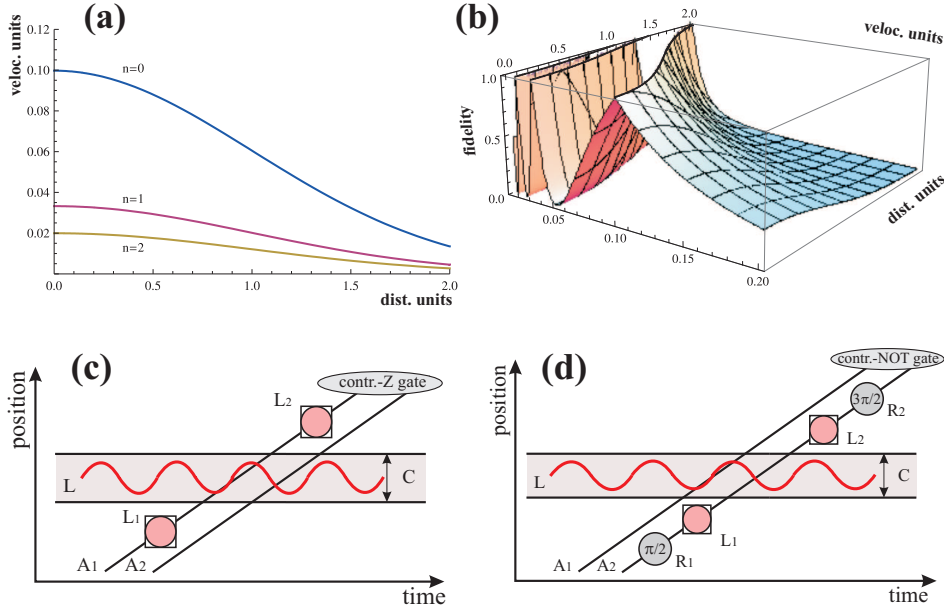


Figure 5. (Color online) (a) Combinations of the atomic velocity v and inter-atomic distance ℓ that realizes the controlled-Z (34) and the controlled-NOT (39) gates, i.e., that satisfy the conditions (36) and (45) for $n = 0, 1, 2$. (b) Fidelity $FCZ(v, \ell)$ as function of the atomic velocity v and inter-atomic distance ℓ . The same units of v and ℓ are used as in Fig. 3. (c) Temporal diagram for generating the controlled-Z gate for the two hyperfine qubits of the atoms A_1 and A_2 . (d) The same as in Fig. 5(c) but for the controlled-NOT gate.

as displayed in Fig. 5(c). The difference between this diagram and the sequence from Fig. 2 is that the second atom A_2 is not subjected to the Raman pulses L_1 and L_2 , implying that its (hyperfine) state $|\bar{0}\rangle$ is not mapped upon the (optical) state $|\bar{a}\rangle$ nor back. Due to suggested setup from Fig. 1(c) this modification, for instance, is realized simply by switching off the pairs of Raman laser beams while the atom A_2 crosses the zones L_1 and L_2 .

Following the temporal sequence in Fig. 5(c) and by making use of Eq. (20), we see that the four input states will evolve (after mapping $|a\rangle \rightarrow |0\rangle$) into

$$\begin{aligned}
 |0, \bar{0}\rangle &\rightarrow |0, \bar{0}\rangle, \\
 |0, \bar{1}\rangle &\rightarrow \cos \theta(v, \ell) |0, \bar{1}\rangle - i \sin \theta(v, \ell) |1, \bar{a}\rangle, \\
 |1, \bar{0}\rangle &\rightarrow |1, \bar{0}\rangle, \\
 |1, \bar{1}\rangle &\rightarrow |1, \bar{1}\rangle.
 \end{aligned} \tag{35}$$

when both atoms passed through the setup. Although the output state in the second line does not belong to the basis set (28), the transformation matrix (34) is obtained whenever the condition

$$\theta(v, \ell) = \pi + 2\pi n, \tag{36}$$

is fulfilled. In this case, the unwanted part $|1, \bar{a}\rangle$ in the second line vanishes. The Fig. 5(a) displays the values of v and ℓ for which the condition (36) is satisfied.

Moreover, by applying the fidelity we introduced in Sec. 3.1, the fidelity between the ideal gate (34) and the effective transformations (35) takes the form

$$F_{CZ}(v, \ell) = 1 - \sqrt{\frac{1 + \cos \theta(v, \ell)}{2}}, \quad (37)$$

and is displayed in Fig. 5(b) for different values of v and ℓ . As for the i-swap gate (29), the least rapid change in the fidelity occurs along the $n = 0$ lines and, in particular, for small interatomic distances but moderate velocities.

3.3. Controlled- $\overline{\text{NOT}}$ Gate

For two interacting qubits A and B , the controlled- $\overline{\text{NOT}}$ gate is defined by the transformation [25]

$$U_{CN} = |0_A\rangle\langle 0_A| \times I^B - |1_A\rangle\langle 1_A| \times U_{\text{not}}^B \quad (38)$$

where $I^B = |0_B\rangle\langle 0_B| + |1_B\rangle\langle 1_B|$ is the identity matrix and $U_{\text{not}}^B = |0_B\rangle\langle 1_B| + |1_B\rangle\langle 0_B|$ denotes the single-qubit NOT gate associated with the qubit B . As for the standard controlled-NOT gate, we shall refer to the qubits A and B as the *control* and *target* qubit, respectively. While the control qubit does not change its state under the gate (38), the target qubit is swapped together with the phase factor $e^{i\pi} = -1$ when the control qubit is set to $|1_A\rangle$. In the basis (28), the controlled- $\overline{\text{NOT}}$ gate is therefore given by the matrix

$$U_{ij}^{CN} = \begin{pmatrix} 1 & 0 & 0 & 0 \\ 0 & 1 & 0 & 0 \\ 0 & 0 & 0 & -1 \\ 0 & 0 & -1 & 0 \end{pmatrix}, \quad (39)$$

where we utilized the assignment

$$|0\rangle = |0_A\rangle, \quad |1\rangle = |1_A\rangle, \quad |\bar{0}\rangle = |0_B\rangle, \quad |\bar{1}\rangle = |1_B\rangle. \quad (40)$$

Obviously, the matrix (39) can not be obtained from the evolutionary matrix (27) by just imposing a single restriction on the coupling angle $\theta(v, \ell)$. Hence we consider the modified temporal diagram displayed in Fig. 5(d). According to this diagram, the control atom A_1 is not subjected to the Raman pulses L_1 and L_2 , however, the target atom A_2 passes through two additional classical microwave fields, in which it undergoes the (coherent) rotation of atomic hyperfine states

$$|\bar{0}\rangle \rightarrow \cos(\eta/2)|\bar{0}\rangle - \sin(\eta/2)|\bar{1}\rangle, \quad (41a)$$

$$|\bar{1}\rangle \rightarrow \sin(\eta/2)|\bar{0}\rangle + \cos(\eta/2)|\bar{1}\rangle, \quad (41b)$$

where the rotation angle η is proportional to the microwave pulse duration. In the literature, such an atom-field interaction is often called a Ramsey pulse and is denoted in Fig. 5(d) by grey circles. These circles contain the interaction time in units of Ramsey rotations η , and the letters R_1 and R_2 are associated with the Ramsey zones in front and behind the cavity [see Fig. 1(c)].

According to Fig. 5(d) and Eqs. (41a)-(41b), the state of A_2 is first transformed

$$|\bar{0}\rangle \xrightarrow{\pi/2} \frac{1}{\sqrt{2}}(|\bar{0}\rangle - |\bar{1}\rangle) \quad \text{or} \quad |\bar{1}\rangle \xrightarrow{\pi/2} \frac{1}{\sqrt{2}}(|\bar{0}\rangle + |\bar{1}\rangle) \quad (42)$$

by using a $\pi/2$ Ramsey pulse in the zone R_1 . Before the atom enters the cavity, the atomic hyperfine state $|\bar{0}\rangle$ is mapped upon the optical state $|\bar{a}\rangle$ by means of the Raman pulse L_1 , which overall, this gives rise to the superposition

$$|\bar{0}\rangle \xrightarrow[L_1]{\pi/2} \frac{1}{\sqrt{2}} (|\bar{a}\rangle - |\bar{1}\rangle) \quad \text{or} \quad |\bar{1}\rangle \xrightarrow[L_1]{\pi/2} \frac{1}{\sqrt{2}} (|\bar{a}\rangle + |\bar{1}\rangle). \quad (43)$$

Inside the cavity, as mentioned above, only the product state $|1, \bar{a}\rangle$ of the two atoms evolves according to Eq. (25). This makes the target qubit A_2 to remain unchanged if the control qubit A_1 was set initially to $|0\rangle$. If the control qubit was set to $|1\rangle$, then the effective atom-atom evolution (25) applies and gives rise to a swap of the target qubit A_2 for a proper choice of the velocity v and the inter-atomic distance ℓ . When both atoms have passed through the cavity, the state $|\bar{a}\rangle$ is mapped back to $|\bar{0}\rangle$ by the Raman pulse L_2 and, finally, the atom A_2 is subjected to a $3\pi/2$ Ramsey pulse in the zone R_2 .

The mentioned Ramsey and Raman pulses together with the cavity and laser field make, therefore, the four input states of the hyperfine qubits to evolve (up to global phase factor)

$$|0, \bar{0}\rangle \rightarrow |0, \bar{0}\rangle, \quad (44a)$$

$$|0, \bar{1}\rangle \rightarrow |0, \bar{1}\rangle, \quad (44b)$$

$$|1, \bar{0}\rangle \rightarrow \frac{(1 + \cos\theta(v, \ell))}{2} |1, \bar{0}\rangle - \frac{(1 - \cos\theta(v, \ell))}{2} |1, \bar{1}\rangle + i \sin\theta(v, \ell) \frac{(|a, \bar{0}\rangle - |a, \bar{1}\rangle)}{2}, \quad (44c)$$

$$|1, \bar{1}\rangle \rightarrow \frac{(1 + \cos\theta(v, \ell))}{2} |1, \bar{1}\rangle - \frac{(1 - \cos\theta(v, \ell))}{2} |1, \bar{0}\rangle + i \sin\theta(v, \ell) \frac{(|a, \bar{0}\rangle - |a, \bar{1}\rangle)}{2}. \quad (44d)$$

Although, again, the output states in the last two lines do not belong entirely to the basis set (28), the matrix (39) can be realized if we impose the condition

$$\theta(v, \ell) = \pi + 2\pi n \quad (45)$$

for the effective coupling angle. Since it is the same condition as Eq. (36) for the controlled-Z gate, the combinations of v and ℓ that are appropriate for the controlled-NOT gate are displayed already in Fig. 5(a) for $n = 0, 1, 2$. The same applies also to the fidelity that is displayed in Fig. 5(b).

4. Summary and Outlook

In summary, a scheme is proposed to generate an entangled state between the hyperfine qubits of two non-interacting four-level atoms being separated by a macroscopical distance. An effective interaction between the atoms is mediated by a detuned optical cavity and a laser beam. The purpose of our work is to analyze how the position-dependent coupling of each atom to the same cavity mode and a laser beam affects the effective interaction among the atoms, and whether it is possible to create a (maximally) entangled state between the atoms. In particular, the analytical expressions for the (asymptotic) coupling angle (21) and the evolutionary matrix (27) tell us explicitly how the degree of entanglement depends on both, the atomic velocity and the (initial) inter-atomic distance. For a position-dependent atom-cavity coupling

(1), these expressions have been derived for the first time for a four-level scheme as described above. In Fig. 3(a), for instance, we have shown that the atom-cavity interaction with a position independent atom-cavity coupling, which was suggested in the Ref. [13], leads to the set of constant atomic velocities for which the maximally entangled state can be generated (see dashed line). Under more realistic assumptions of position-dependent atom-cavity coupling, however, these velocities are not constant but depend on the values of inter-atomic distance according to expression (21). From Fig. 3(b), moreover, it can be seen how sensitive the entanglement depends on variations in these parameters, an important requisite for any experimental realization. Finally, a few realistic schemes are suggested to implement some basic two-qubit quantum gates, such as i-swap gate, controlled-Z, and the controlled- $\overline{\text{NOT}}$ gate in the framework of the given cavity-laser setup. For all these schemes, we displayed the atomic velocities and inter-atomic distances for which these gates are realized, i.e., the gate fidelities become maximal.

Following the recent experiments [26, 20, 21] and the theoretical works of Refs. [18, 27, 28, 29], the position-dependent effects on the effective atom-atom interaction and entanglement formation mediated by a (detuned) optical cavity, are acknowledged today as a notable step in obtaining the control over the entanglement of atoms within the framework of cavity QED. In particular, Li and coworkers [18] suggested that the distance between the atoms is an important parameter that can be utilized to control the (position-dependent) atom-cavity coupling which implies also the control over the atomic entanglement. Instead of using a two-level atomic configuration, however, for the cavities in optical domain it appears more suitable to consider a four-level Λ -type level configuration in which the quantum information is stored in the hyperfine levels of the atomic ground state. Such a configuration appears to be essential for the recent experimental attempts [19, 20, 21] in which atoms are transported coherently inside the cavity by means of an optical lattice trap (conveyor belt). For such a belt, the inter-atomic distance is given by the wavelength of the (standing) optical lattice, while the velocity of the atoms is set by a shift in the frequencies of the counter-propagating laser beams.

A further extension of the effective atom-atom evolution as described in Sec. 2, might be a chain of N four-level atoms that cross the experimental setup in Fig. 1(c) and interacts simultaneously with the same cavity mode while passing through the cavity. This extension would lead naturally to the generation of various N -partite entangled states depending on the (v, ℓ) regime and the succession of Raman and Ramsey zones (see for instance Ref. [30], where we discussed the formation of genuine entangled states for a chain of N bi-level atoms which cross an analogous experimental set-up we considered in this paper). Finally we remark that a realistic atom-cavity interaction evolution should also include the decoherence effects, which have been avoided in this paper so far. We note that in order to analyze the time evolution of such quantum systems embedded into a reservoir or under the external noise and to analyze different entanglement or separability measures, including those in Eqs. (23) and (31), a quantum simulator has been developed recently in our group [31] that can be utilized for such studies in future.

Acknowledgments

This work was supported by the DFG under the project No. FR 1251/13.

References

- [1] Bennett C H and Wiesner S J 1992 *Phys. Rev. Lett.* **69** 2881
- [2] Ekert A K 1991 *Phys. Rev. Lett.* **67** 661
- [3] Grover L K 1997 *Phys. Rev. Lett.* **79** 325
- [4] Rempe G 1993 *Contemp. Phys.* **34** 119
- [5] Kimble H J 1998 *Physica Scripta* **T76** 127
- [6] Vahala K J 2003 *Nature* **424** 838
- [7] Treutlein P, Hommelhoff P, Steinmetz T, Hänsch T W, and Reichel J 2004 *Phys. Rev. Lett.* **92** 203005
- [8] Langer C et al. 2005 *Phys. Rev. Lett.* **95** 060502
- [9] Kuhr S et al. 2003 *Phys. Rev. Lett.* **91** 213002
- [10] Schrader D et al. 2004 *Phys. Rev. Lett.* **93** 150501
- [11] Jones M P A et al. 2007 *Phys. Rev. A* **75** 040301(R)
- [12] Olmschenk S et al. 2007 *Phys. Rev. A* **76** 052314
- [13] You L, Yi X X, and Su X H 2003 *Phys. Rev. A* **67** 032308
- [14] Zheng S B and Guo G C 2000 *Phys. Rev. Lett.* **85** 2392
- [15] Osnaghi S et al. 2001 *Phys. Rev. Lett.* **87** 037902
- [16] Shen Y R 1967 *Phys. Rev.* **155** 921
- [17] Sørensen A and Mølmer K 1999 *Phys. Rev. Lett.* **82** 1971
- [18] Li Y, Bruder C, and Sun C P 2007 *Phys. Rev. A* **75** 032302
- [19] Fortier K M, Kim S Y, Gibbons M J, Ahmadi P, and Chapman M S 2007 *Phys. Rev. Lett.* **98** 233601
- [20] Nussmann S et al. 2005 *Phys. Rev. Lett.* **95** 173602
- [21] Khudaverdyan M et al. 2008 *New J. Phys.* **10** 073023
- [22] Nielsen M A and Chuang I L 2000 *Quantum Computation and quantum Information* (Cambridge: Cambridge University Press)
- [23] Schuch N and Siewert J 2003 *Phys. Rev. A* **67** 032301
- [24] Golub G H and Van Loan C F 1996 *Matrix Computations* (Baltimore: Johns Hopkins)
- [25] In contrast to the controlled- $\overline{\text{NOT}}$ gate we have defined in Eq. (38), the conventional controlled-NOT gate [22]: $U = |0_A\rangle\langle 0_A| \times I^B + |1_A\rangle\langle 1_A| \times U_{\text{not}}^B$ implies only the flipping of the target qubit (without accumulating a phase) when the control qubit is set to $|1_A\rangle$.
- [26] Pachos J K and Walther H 2002 *Phys. Rev. Lett.* **89** 187903
- [27] Asbóth J K, Domokos P, and Ritsch H 2004 *Phys. Rev. A* **70** 013414
- [28] Natali S and Ficek Z 2007 *Phys. Rev. A* **75** 042307
- [29] Lazarou C and Garraway B M 2008 *Phys. Rev. A* **77** 023818
- [30] Gonta D, Fritzsche S, and Radtke T 2008 *Phys. Rev. A* **77** 062312
- [31] Radtke T and Fritzsche S 2006 *Comput. Phys. Commun.* **175** 145